

Stability and Bifurcation Analysis of Planar Piecewise Affine Systems ^{*}

Takuya Iwaki ^{*} Tomohisa Hayakawa ^{*}

^{*}Department of Mechanical and Environmental Informatics
Tokyo Institute of Technology
Tokyo 152-8552, JAPAN (e-mail: hayakawa@mei.titech.ac.jp).

Abstract: In this paper, stability and bifurcation of piecewise affine systems is investigated. In the stability analysis, stability of the origin and existence of limit cycles are investigated by means of the radial growth rate, which describes the behavior of the radial direction of the trajectories. In the bifurcation analysis, Hopf bifurcation and saddle-node bifurcation is discussed. The radial growth rate is also used for characterizing the return map in the discussion.

Keywords: Nonlinear systems, piecewise affine systems, stability analysis, Lyapunov function, limit cycles, bifurcations

1. INTRODUCTION

In this paper, stability and bifurcation of piecewise affine systems are investigated. Piecewise affine systems are applied as a mathematical model to various kinds of phenomena in the nature and our society (see, for example, Farcot et al. (2010), Kashima et al. (2010), and Varela et al. (2008)). For instance, in Farcot et al. (2010) and Kashima et al. (2010), periodic behavior in the organism is modeled by piecewise affine systems, and in Varela et al. (2008), piecewise affine systems are used to express the oscillation of economical situation.

In this paper, we focus on planar piecewise affine systems whose 2-dimensional state space is partitioned by conewise domains from the origin. Stability problems of this type of piecewise linear and affine systems have been attracting in Johansson (2003) and Nishiyama et al. (2008). Furthermore, bifurcation analysis of conewise linear and affine systems are investigated in Biomond et al. (2009), Zou et al. (2005), and Akhmet et al. (2009). Specifically, in Nishiyama et al. (2008), a novel framework of determining stability of piecewise linear systems is developed. Nishiyama et al. (2008) introduce the integral of growth rate to determine the stability of piecewise linear systems. The integral of radial growth rate is the function which characterizes how far the trajectories move to radial direction along the elapse of time. In the discussion of stability and bifurcation of piecewise affine systems in this paper, the integral of radial growth rate is used as a key function.

In the stability analysis of piecewise affine systems, we present the way to check stability of the origin and the existence condition of limit cycles. For stability of the origin, we configure Lyapunov function by means of the integral of radial growth rate. Furthermore, for the discussion of existence of limit cycles, we apply the idea of Poincaré-Bendixson Theorem described in Strogatz (2001) which is generally used for nonlinear dynamical systems to check the existence of limit

cycles. In this discussion, the integral of radial growth rate is also used to determine the existence of invariant, bounded, and closed set which is necessary for Poincaré-Bendixson Theorem to guarantee the existence of limit cycles.

In the discussion of bifurcation of piecewise affine systems, we investigate Hopf bifurcation of the equilibrium point and saddle-node bifurcation of the limit cycles. We observe the process of bifurcation by means of the integral of radial growth rate which characterizes a return map.

This paper is organized as follows. In Section 2, the definition of the radial growth rate and its important property are given. In Section 3, the definition of piecewise affine systems are given. Furthermore, piecewise linear and constant systems and their radial growth rate are defined as a preparation of the stability analysis of piecewise affine systems in the next section. In Section 4, stability of the origin and existence of the limit cycles of piecewise affine systems are discussed. In Section 5, bifurcation analysis with numerical example is conducted. Finally, conclusion is stated in Section 6.

2. MATHEMATICAL PRELIMINARIES

In this section, we introduce notation, several definitions, and some key results concerning planar nonlinear dynamical systems that are necessary for developing the main results of this paper. Specifically, consider the planar nonlinear dynamical system given by

$$\dot{x}(t) = f(x(t)), \quad x(t) \in \mathcal{D}, \quad x(0) = x_0, \quad t \geq 0, \quad (1)$$

where $x(t) = [x_1(t), x_2(t)]^T \in \mathbb{R}^2$ is the state vector. Furthermore, consider the polar form (r, θ) of the coordinate $[x_1, x_2]^T$, where r is the distance from the origin and θ is the angle (phase) from the positive x_1 -axis in the counter-clockwise direction.

2.1 Rotational Direction of Trajectories

The rotational direction of the trajectories of (1) at x can be determined by examining the sign of $d\theta/dt$; that is, $d\theta/dt > 0$ (resp., $d\theta/dt < 0$) implies that the trajectories of (1) is moving in counter-clockwise (resp., clockwise) direction at x .

^{*} This research is supported in part by Aihara Innovative Mathematical Modelling Project, the Funding Program for World-Leading Innovative R&D on Science and Technology (FIRST Program) from Japan Society for the Promotion of Science(JSPS).

Assume that the nonlinear dynamical systems (1) has the equilibrium point at the origin, that is, $f(0) = 0$, and elsewhere the state moves only in the counter-clockwise direction. Under these assumptions, we can convert the nonlinear dynamical system (1) to the polar form given by

$$\begin{cases} \dot{r}(t) &= f_r(r(t), \theta(t)), \quad r(0) = r_0, \quad t \geq 0, \\ \dot{\theta}(t) &= f_\theta(r(t), \theta(t)), \quad \theta(0) = \theta_0. \end{cases} \quad (2)$$

Again, we assume that $\dot{\theta}(t) > 0$, $t \geq 0$, is satisfied.

2.2 Radial Growth Rate

Radial growth rate is in general the function of (r, θ) defined in Nishiyama et al. (2008) to characterize the stability of piecewise linear systems. In this paper, we apply the radial growth rate to the nonlinear dynamical system (1) and develop a proposition in order to discuss stability and bifurcation of piecewise affine systems.

Now, consider the polar form of the nonlinear dynamical system (2). For this system, the radial growth rate is defined by

$$\rho(r, \theta) \triangleq \frac{1}{r} \frac{dr}{d\theta}. \quad (3)$$

Here, we consider the integral of the radial growth rate along the trajectories of the system (2). Note that the position of the trajectories at time t can be determined if initial value $[r_0, \theta_0]^T$ is given. We describe the trajectories at time t with the initial value $[r_0, \theta_0]^T$ as $[r(t; r_0, \theta_0), \theta(t; r_0, \theta_0)]^T$. Furthermore, the trajectories of the nonlinear dynamical system (2) always move in counter-clockwise direction, so that the phase θ can be uniquely determined according to time t and the initial value $[r_0, \theta_0]^T$. Therefore, $r(t; r_0, \theta_0)$ can be described as $r(\theta; r_0, \theta_0)$ instead. Since $r(t)$ can be determined from phase θ and the initial value (r_0, θ_0) , the radial growth rate $\rho(r(t), \theta(t))$ can also be given by θ and $[r_0, \theta_0]^T$ and hence, it can be described as $\rho(\theta; r_0, \theta_0)$.

The integral of the radial growth rate from θ_0 to $\theta_0 + 2\pi$ is defined as the function of $[r_0, \theta_0]^T$ by

$$\Gamma(r_0, \theta_0) \triangleq \int_{\theta_0}^{\theta_0 + 2\pi} \rho(\theta; r_0, \theta_0) d\theta. \quad (4)$$

This function $\Gamma(r_0, \theta_0)$ represents how far the trajectory is going from the origin when the state travels and make one round from a point $[r_0, \theta_0]^T$ back to another point with the same phase θ_0 . Now, we present the proposition about the property of the integral of radial growth rate.

Proposition 1. Consider the nonlinear dynamical system (2). Then the integral of the radial growth rate (4) satisfies

$$\Gamma(r_0, \theta_0) = \log \frac{r(\theta_0 + 2\pi; r_0, \theta_0)}{r_0}, \quad (5)$$

that is, the following statements hold:

- If $\Gamma(r_0, \theta_0) < 0$, then $r(\theta_0 + 2\pi; r_0, \theta_0) < r_0$;
- If $\Gamma(r_0, \theta_0) = 0$, then $r(\theta_0 + 2\pi; r_0, \theta_0) = r_0$ and the trajectories of (2) are closed orbits;
- If $\Gamma(r_0, \theta_0) > 0$, then $r(\theta_0 + 2\pi; r_0, \theta_0) > r_0$.

Proof. The result is immediate from (4) and

$$\begin{aligned} \Gamma(r_0, \theta_0) &= \int_{\theta_0}^{\theta_0 + 2\pi} \frac{1}{r(\theta; r_0, \theta_0)} \frac{dr}{d\theta} d\theta \\ &= \int_{r_0}^{r(\theta_0 + 2\pi; r_0, \theta_0)} \frac{dr}{r} \\ &= \log \frac{r(\theta_0 + 2\pi; r_0, \theta_0)}{r_0}. \end{aligned} \quad (6)$$

□

Proposition 1 indicates that the integral of the radial growth rate characterizes whether the trajectories of (2) are approaching to the origin along the elapse of time. By plotting the value of $\Gamma(r_0, \theta_0)$ versus r_0 , we can observe the behavior of the trajectories of (2). For instance, if $\Gamma(r_0, \theta_0)$ crosses the line of $\Gamma(r_0, \theta_0) = 0$, we find the fixed point here, hence the limit cycle exists on that point. In this way, the integral of radial growth rate can be used as an return map. We discuss the bifurcation of piecewise affine systems in Section 5 based on this idea.

3. PIECEWISE PLANAR AFFINE SYSTEMS

In this section, we introduce planar piecewise affine systems and discuss stability by utilizing the radial growth rate.

First, consider the piecewise affine (PWA) system given by

$$\dot{x}(t) = A_i x(t) + b_i, \quad x(t) \in \mathcal{D}_i, \quad x(0) = x_0, \quad t \geq 0, \quad (7)$$

where $x(t) = [x_1(t), x_2(t)]^T \in \mathbb{R}^2$ is the state vector, $A_i \in \mathbb{R}^{2 \times 2}$, $b_i \in \mathbb{R}^2$, $i \in \{0, 1, \dots, k\}$ are a system matrix and a constant vector, respectively, that we allowed to assign to the domain \mathcal{D}_i , and k is the number of domains (modes) which the state space is partitioned into. Here, the domains \mathcal{D}_i , $i = 1, \dots, k$, are assumed to satisfy

$$\bigcup_{i=0}^k \mathcal{D}_i = \mathbb{R}^2, \quad (8)$$

$$\text{int}(\mathcal{D}_i) \cap \text{int}(\mathcal{D}_j) = \emptyset, \quad i, j = 0, \dots, k, \quad i \neq j. \quad (9)$$

In this paper, we also assume that the state space is partitioned by semi-infinite straight lines originating from the origin such that

$$\mathcal{D}_i \triangleq \{c_i e(\theta_i) + d_i e(\theta_{i+1}) : c_i, d_i \geq 0\}, \quad i = 1, \dots, k, \quad (10)$$

$$\mathcal{D}_0 \triangleq \{0\}, \quad (11)$$

where $c_i, d_i \in \mathbb{R}$, $\theta_i \in [0, 2\pi)$, $e(\theta_i) \triangleq [\cos \theta_i, \sin \theta_i]^T$ characterizes the i th semi-infinite partitioning straight line. Furthermore, we assume $\theta_{k+1} = \theta_1$ and $A_i x \neq 0$, $x \in \mathcal{D}_i$, $b_i \neq 0$, $i = 1, \dots, k$. In addition, to guarantee that the origin be an equilibrium point, we assume that $A_0 = 0$, $b_0 = 0$ are satisfied at \mathcal{D}_0 . Fig. 1 shows an example of piecewise planar affine systems in case of $k = 4$.

Next, we define piecewise linear (PWL) systems and piecewise constant (PWC) systems for the discussion in this paper given by

$$\dot{x}(t) = A_i x(t), \quad x(t) \in \mathcal{D}_i, \quad x(0) = x_0, \quad t \geq 0, \quad (12)$$

$$\dot{x}(t) = b_i, \quad x(t) \in \mathcal{D}_i, \quad x(0) = x_0, \quad t \geq 0, \quad (13)$$

respectively. The integral of the radial growth rate of (12) and (13) given in Section 3.2 are the key values in the discussion of stability of the original PWA system (7).

3.1 Rotational Direction of PWA, PWL, and PWC Systems

In this paper, we assume that the trajectories of the PWA system (7), the PWL system (12), and the PWC system (13) are always

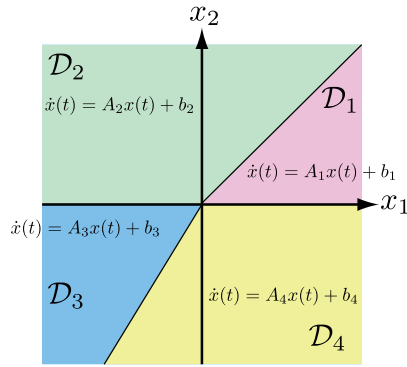


Fig. 1. Planar piecewise affine systems

in counter-clockwise direction: that is, for the PWA system (7),

$$\dot{\theta}(t) = -e^T(\theta(t))GA_i e(\theta(t)) - \frac{1}{r(t)}e^T(\theta(t))Gb_i > 0, \quad t \geq 0, \quad \theta \in [\theta_i, \theta_{i+1}), \quad i = 1, \dots, k, \quad (14)$$

is assumed. Specifically, for further discussion, we assume that the parameters of the PWA system (7), the PWL system (12), and the PWC system (13) satisfy the following statement.

Assumption 2. The PWA system (7) and the PWL system (12) satisfy

$$e^T(\theta)GA_i e(\theta) < 0, \quad \theta \in [\theta_i, \theta_{i+1}), \quad i = 1, \dots, k, \quad (15)$$

and the PWA system (7) and the PWC system (13) satisfy

$$e^T(\theta)Gb_i < 0, \quad \theta \in [\theta_i, \theta_{i+1}), \quad i = 1, \dots, k, \quad (16)$$

where

$$e(\theta) \triangleq [\cos \theta, \sin \theta]^T, \quad (17)$$

$$G \triangleq \begin{bmatrix} 0 & -1 \\ 1 & 0 \end{bmatrix}. \quad (18)$$

Under this assumption, we guarantee that the rotational direction of the trajectories is in the counter-clockwise direction so that we avoid intricate issues concerning existence and uniqueness of solutions of the PWA, the PWL, and the PWC systems.

3.2 Radial Growth Rate of PWL and PWC systems

To discuss the stability of the PWA system (7), the radial growth rate of the PWL system (12) and the PWC system (13) associated with (7) are introduced. From the discussion in Nishiyama et al. (2008), the radial growth rate of the PWL system

$$\rho_A(\theta) \triangleq \frac{1}{r} \frac{dr}{d\theta} \quad (19)$$

$$= -\frac{e^T(\theta)A_i e(\theta)}{e^T(\theta)GA_i e(\theta)}, \quad \theta \in [\theta_i, \theta_{i+1}), \quad i = 1, \dots, k, \quad (20)$$

depends solely on θ but r . Note that the function $\rho_A(\theta)$ is periodic of period 2π .

By integrating the radial growth rate given by (20) from θ_0 to $\theta_0 + 2\pi$, we obtain the integral of the radial growth rate for the PWL system (12). Since (20) is a function of only θ , the integral of the radial growth rate defined by

$$\Gamma_A \triangleq \int_{\theta_0}^{\theta_0+2\pi} \rho_A(\theta) d\theta = \int_0^{2\pi} \rho_A(\theta) d\theta, \quad (21)$$

is constant for any given $[r_0, \theta_0]^T$. From this fact and Proposition 1, we present one of the ways to check whether the PWL system (12) is stable as derived in Nishiyama et al. (2008).

Proposition 3. Consider the PWL system given by (12), and the integral of the radial growth rate (21). Then the following statements hold:

- If $\Gamma_A < 0$, then (12) is globally asymptotically stable;
- If $\Gamma_A = 0$, then (12) is marginally stable and trajectory of (12) constitutes a closed orbit;
- If $\Gamma_A > 0$, then (12) is unstable.

For the PWC systems (13), the radial growth rate can be evaluated in the same way defined by

$$\rho_b(\theta) \triangleq \frac{1}{r} \frac{dr}{d\theta} \quad (22)$$

$$= -\frac{e^T(\theta)b_i}{e^T(\theta)Gb_i}, \quad \theta \in [\theta_i, \theta_{i+1}), \quad i = 1, \dots, k. \quad (23)$$

Note that the radial growth rate of the PWC system (13) depends also solely θ but r , so that we present the proposition with the integral of the radial growth rate as well.

Proposition 4. Consider the PWC system given by (13), and the integral of the radial growth rate from θ_0 to $\theta_0 + 2\pi$,

$$\Gamma_b \triangleq \int_{\theta_0}^{\theta_0+2\pi} \rho_b(\theta) d\theta = \int_0^{2\pi} \rho_b(\theta) d\theta. \quad (24)$$

Then the following statements hold:

- If $\Gamma_b < 0$, then (13) is globally asymptotically stable;
- If $\Gamma_b = 0$, then (13) is marginally stable and trajectory of (13) constitutes a closed orbit;
- If $\Gamma_b > 0$, then (13) is unstable.

4. STABILITY ANALYSIS OF PWA SYSTEMS

In this section, stability of the origin and existence of a limit cycle is discussed. In this discussion, the integral of the radial growth rate of the PWL system (21) and the PWC system (24) are used.

4.1 Stability of the Origin

In the neighborhood of the origin, constant vector term b_i of the PWA system (7) is dominant to determine the behavior of the trajectory since $\|x(t)\|$ becomes small in the neighbourhood of the origin. Therefore, Γ_b is used to characterize the stability of the PWA system (7).

Now, we present the way to check the stability of the PWA system (7).

Theorem 5. Consider the PWA system given by (7) which satisfy Assumption 2. Then the following statements hold:

- If $\Gamma_b < 0$, then (7) is asymptotically stable;
- If $\Gamma_b > 0$, then (7) is unstable.

Furthermore, if

$$\Gamma_b \leq 0, \quad (25)$$

and

$$\rho_A(\theta) - \rho_b(\theta) > -\frac{\Gamma_b}{2\pi}, \quad \theta \in [0, 2\pi), \quad (26)$$

then (7) is globally asymptotically stable.

From Theorem 5, we can check stability of the PWA system by calculating Γ_b . Generally, for the nonlinear dynamical system,

stability is characterized by Jacobian of the system at the equilibrium point. However, Jacobian of the PWA system (7) cannot be defined due to the discontinuity at the switching lines. Hence, Γ_b is used to characterize stability instead of Jacobian.

4.2 Existence of Limit Cycle

Next, we discuss existence of a limit cycles of the PWA system (7). The PWA system (7) can have the limit cycles in spite of its linearity of affine term, and this is one of the features of this system.

Generally, to discuss existence of the limit cycles for the continuous nonlinear system, Poincaré-Bendixson Theorem is used. In this paper, extended Poincaré-Bendixson Theorem for the PWA system (7) is presented.

Lemma 6. Consider the PWA system (7) with Assumption 2. If the PWA system (7) satisfies the following statements:

- There exists an invariant, bounded, and closed set $\mathcal{M} \in \mathbb{R}^2$.
- There is no equilibrium point in \mathcal{M} .

then the PWA system (7) has stable limit cycles.

From this lemma, if we can guarantee existence of the invariant, bounded, and closed set, we obtain the condition of existence of the limit cycles for the PWA system (7). To derive the condition of existence of the invariant, bounded, and closed set, first we present the condition of boundedness for the PWA system (7).

Lemma 7. Consider the PWA system given by (7) which satisfy Assumption 2. Then if $\Gamma_A < 0$, the PWA system (7) is bounded.

From this lemma and Theorem 5, we are finally ready to state one of the main results of this paper.

Theorem 8. Consider the PWA system (7) with Assumption 2. If the PWA system (7) satisfies $\Gamma_A < 0$ and $\Gamma_b > 0$, then there exist limit cycles for PWA system (7).

5. BIFURCATION OF PWA SYSTEMS

In this section, we discuss bifurcation of the PWA systems with a bifurcation parameter. Specifically, consider the PWA system

$$\dot{x}(t) = A_i x(t) + b_i(\mu), \quad x(t) \in \mathcal{D}_i, \quad x(0) = x_0, \quad t \geq 0, \quad (27)$$

where $\mu \in [\mu_1, \mu_2]$, $\mu_1, \mu_2 \in \mathbb{R}$, is bifurcation parameter. Furthermore, assume that the trajectories of the PWA system satisfy (15) and (16) for any $\mu \in [\mu_1, \mu_2]$ to guarantee that the state moves in the counter-clockwise direction of the trajectories.

To observe the process of bifurcation of the system (27), the integral of the radial growth rate is used. First, we derive the radial growth rate of the PWA system (27). Note that the dynamics of $r(t)$ for the PWA system (27) is given by

$$\dot{r}(t) = r(t)e^T(\theta(t))A_i e(\theta(t)) + e^T(\theta(t))b_i(\mu), \quad \theta \in [\theta_i, \theta_{i+1}), \quad i = 1, \dots, k. \quad (28)$$

Then the radial growth rate of the PWA system (27) is defined from (14) and (28) by

$$\rho(r, \theta) = \lambda_i(r, \theta)\rho_A(\theta) + (1 - \lambda_i(r, \theta))\rho_b(\theta, \mu), \quad \theta \in [0, 2\pi), \quad i = 1, \dots, k, \quad (29)$$

where

$$\lambda_i(r, \theta, \mu) \triangleq \frac{re^T(\theta)GA_i e(\theta)}{re^T(\theta)GA_i e(\theta) + e^T(\theta)Gb_i(\mu)}. \quad (30)$$

Finally, by integrating (29) from θ_0 to $\theta_0 + 2\pi$ along the trajectory of (27), the integral of the radial growth rate for the PWA system (27)

$$\Gamma(r_0, \theta_0, \mu) = \int_{\theta_0}^{\theta_0+2\pi} \left\{ \lambda_i(\theta, \mu; r_0, \theta_0)\rho_A(\theta) + (1 - \lambda_i(\theta, \mu; r_0, \theta_0))\rho_b(\theta, \mu) \right\} d\theta, \quad \theta \in [\theta_i, \theta_{i+1}), \quad i = 1, \dots, k, \quad (31)$$

is derived.

5.1 Hopf Bifurcation

Now, consider the PWA system (27). If $\Gamma_b(\mu)$ is changed from negative to positive (resp., positive to negative) along the change of μ , stability of the PWA system also changes unstable (resp., stable), then stable limit cycle appears or unstable limit cycle disappears (resp., unstable limit cycle appears or stable limit cycle disappears) around the origin. Here, Hopf bifurcation can be observed when the value of μ crosses 0. In the following discussion, we present two examples of Hopf bifurcation: supercritical Hopf bifurcation and degenerate Hopf bifurcation.

First, we show the supercritical Hopf bifurcation. In this bifurcation, the stable equilibrium point becomes unstable and stable limit cycle appears when the value of μ crosses a threshold. Assume that we are given the system parameters

$$\begin{aligned} A_1 = A_5 &= \begin{bmatrix} -1 & -5 \\ 1 & 0 \end{bmatrix}, & A_2 = A_6 &= \begin{bmatrix} 0 & -5 \\ -1 & -1 \end{bmatrix}, \\ A_3 = A_7 &= \begin{bmatrix} 0 & -1 \\ 5 & -1 \end{bmatrix}, & A_4 = A_8 &= \begin{bmatrix} -1 & 1 \\ 5 & 0 \end{bmatrix}, \\ b_1 = b_8 &= \begin{bmatrix} \mu \\ 5 \end{bmatrix}, & b_2 = b_3 &= \begin{bmatrix} -5 \\ \mu \end{bmatrix}, \\ b_4 = b_5 &= \begin{bmatrix} \mu \\ -5 \end{bmatrix}, & b_6 = b_7 &= \begin{bmatrix} 5 \\ -\mu \end{bmatrix}, \end{aligned}$$

where the partitioning angle is $\theta_i = \frac{\pi}{4}i$, $i = 1, \dots, 8$. Furthermore, note that the parameters yield trajectories moving counter-clockwise direction in $\mu \in [-5, 5]$, and $\Gamma_A = -8.01$, $\Gamma_b(-1) = -1.03$, $\Gamma_b(0) = 0$, and $\Gamma_b(1) = 1.03$. Then it follows from Theorems 5 and 8 that when μ changes positive from negative, the stable origin bifurcates to be the unstable origin and the stable limit cycle. Now, plot the trajectory of the system as in Figs. 2, 4, 6 and the value of $\Gamma(r_0, 0)$ versus r_0 as in Figs. 3, 5, 7. When $\mu = -1$, the system is stable from Theorem 5. The trajectory shown in Fig 2 converges to the origin and $\Gamma(r_0, 0)$ is negative as in Fig. 3. When $\mu = 0$, the trajectory of the system is still converging to the origin as shown in Figs. 4 and 5. However, when $\mu = 1$, the origin of the system is unstable and the stable limit cycle appears around it. Existence of the limit cycle is guaranteed by Theorem 8 since $\Gamma_A < 0$ and $\Gamma_b(1) > 0$. In Fig. 6, there exist an intersection of $\Gamma(r_0, 0)$ and r_0 -axis around $r_0 = 0.5$. Furthermore, we find the trajectory which converges to the closed orbit in Fig. 7.

Second, we show the degenerate Hopf bifurcation [Strogatz (2001)]. Assume that we are given the system parameters

$$\begin{aligned} A_1 = A_3 = A_5 = A_7 &= \begin{bmatrix} 2 & -3 \\ 3 & 2 \end{bmatrix}, \\ A_2 = A_4 = A_6 = A_8 &= \begin{bmatrix} -2 & -3 \\ 3 & -2 \end{bmatrix}, \end{aligned}$$

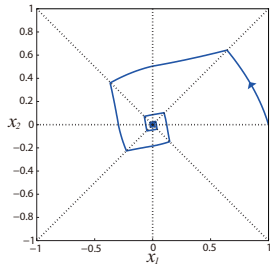


Fig. 2. Phase portrait ($\mu = -1$)

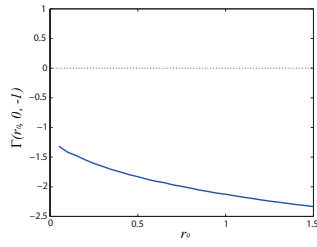


Fig. 3. Integral of radial growth rate versus r_0 ($\mu = -1$)

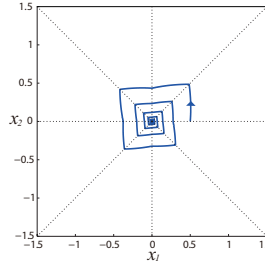


Fig. 8. Phase portrait ($\mu = -0.8$)

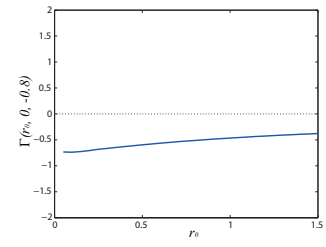


Fig. 9. Integral of radial growth rate versus r_0 ($\mu = -0.8$)

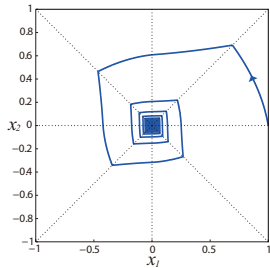


Fig. 4. Phase portrait ($\mu = 0$)

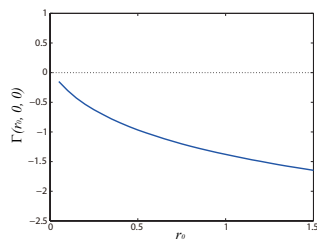


Fig. 5. Integral of radial growth rate versus r_0 ($\mu = 0$)

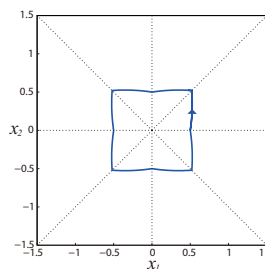


Fig. 10. Phase portrait ($\mu = 0$)

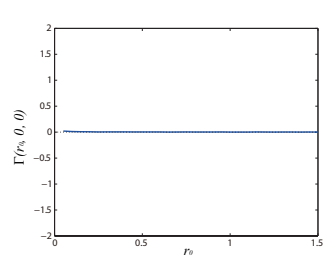


Fig. 11. Integral of radial growth rate versus r_0 ($\mu = 0$)

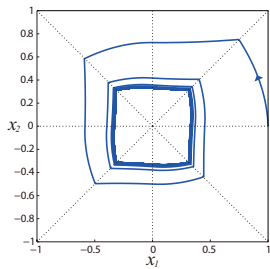


Fig. 6. Phase portrait ($\mu = 1$)

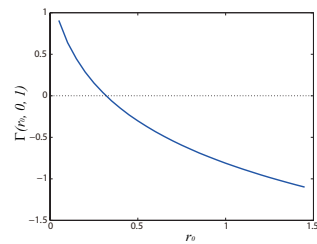


Fig. 7. Integral of radial growth rate versus r_0 ($\mu = 1$)

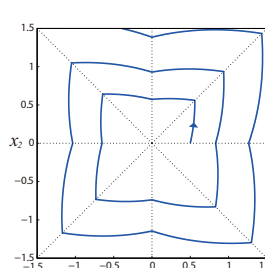


Fig. 12. Phase portrait ($\mu = 0.8$)

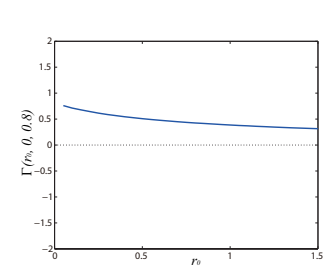


Fig. 13. Integral of radial growth rate versus r_0 ($\mu = 0.8$)

$$b_1 = b_8 = \begin{bmatrix} \mu \\ 5 \end{bmatrix}, \quad b_2 = b_3 = \begin{bmatrix} -5 \\ \mu \end{bmatrix},$$

$$b_4 = b_5 = \begin{bmatrix} \mu \\ -5 \end{bmatrix}, \quad b_6 = b_7 = \begin{bmatrix} 5 \\ -\mu \end{bmatrix},$$

where the partitioning angle is $\theta_i = \frac{\pi}{4}i$, $i = 1, \dots, 8$. Note that $\Gamma_A = 0$, $\Gamma_b(-0.8) = -0.82$, $\Gamma_b(0) = 0$, $\Gamma_b(0.8) = 0.82$. Now, plot the trajectory of the system as in Figs. 8, 10, 12 and the value of $\Gamma(r_0, 0)$ versus r_0 as in Figs. 9, 11, 13. When $\mu = -0.8$, the system is stable from Theorem 5. The trajectory shown in Fig. 8 converges to the origin and $\Gamma(r_0, 0)$ is negative as in Fig. 9. When $\mu = 0$, trajectory of the system becomes closed orbit, as shown in Fig. 4. Furthermore, we also find that the origin is marginally stable from Fig. 5. However, when $\mu = 0.8$, the origin of the system is unstable and the closed orbits disappear. The trajectory shown in Fig. 12 is unstable and $\Gamma(r_0, 0)$ is positive as in Fig. 9.

5.2 Saddle-Node Bifurcation of PWA Systems

If the PWA system (27) has multiple limit cycles, saddle-node bifurcation of the limit cycles can be observed. Now, assume that we are given the parameters

$$A_1 = A_3 = \begin{bmatrix} -1 & -5 \\ 1 & 0 \end{bmatrix}, \quad A_2 = A_4 = \begin{bmatrix} 0 & -10 \\ -20 & -10 \end{bmatrix},$$

where the partitioning angle is $\theta_i = \frac{\pi}{2}i$, $i = 1, \dots, 4$. In this case, when $\mu = 50$, there exist two intersecting points between $\Gamma(r_0, 0)$ and r_0 -axis as in Fig. 14, so that we find two limit cycles (inner one is unstable and the other is stable). As μ decreases, we find that the two limit cycles are approaching each other and finally they collide and one saddle-type limit cycle appears as in Fig. 15. Furthermore, when μ continues to decrease, the limit cycle disappears as in Fig. 16.

6. CONCLUSION

In this paper, we investigated stability of the PWA system (7). In this discussion, we proposed how to check stability of the origin and present the existence condition of the limit cycles. To check stability of the origin, the integral of the radial growth rate of the PWC system is used since the behavior of the PWA system is dominated by constant term. Existence of the limit cycles is discussed based on the idea of Poincaré Bendixon theorem. In addition, existence of the invariant, bounded, and closed set is guaranteed by the integral of the radial growth rate of the PWC system and the PWL system.

Furthermore, we investigated bifurcation of the PWA system (27). In particular, Hopf bifurcation of the origin and saddle-

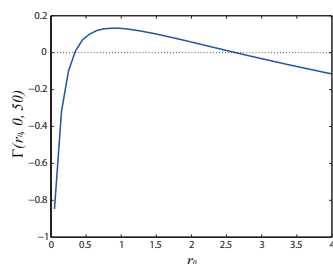


Fig. 14. Integral of radial growth rate versus r_0 ($\mu = 50$)

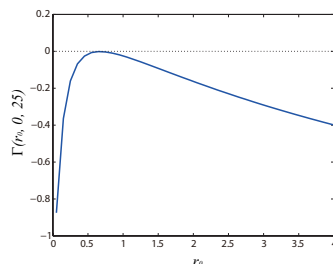


Fig. 15. Integral of radial growth rate versus r_0 ($\mu = 25$)

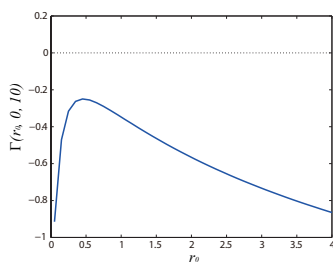


Fig. 16. Integral of radial growth rate versus r_0 ($\mu = 10$)

node bifurcation of the limit cycles are observed by means of the integral of the radial growth rate. The radial growth rate of PWA systems is used for characterizing the return map in this discussion.

Future extensions include applying more general class of piecewise smooth systems.

REFERENCES

- E. Farcot and J. Gouzé. Limit cycles in piecewise-affine gene network models with multiple interaction loops. *Int. J. of Systems Science*, volume 41, pp. 119-130, 2010.
- K. Kashima, Y. Kawamura, and J. Imura. Oscillation analysis of linearly coupled piecewise affine systems: Application to spatio-temporal neuron dynamics. *Automatica*, Vol. 47, No. 6, pp. 1249-1254, 2011.
- A. A. S. Varela, G. B. Stan, and J. Goncalves. Global asymptotic stability of the limit cycle in piecewise linear versions of the Goodwin oscillator. *IFAC World Cong.*, pp. 6-11, 2008
- M. Johansson. *Piecewise Linear Control Systems*. Springer-Verlag, 2003.
- S. Nishiyama and T. Hayakawa. Optimal stable state-space partitioning for piecewise linear planer systems. *Proc. Amer. Contr. Conf.*, pp. 3959-3965, 2008.
- B. Biemond, N. Wouw, and H. Nijmeijer. A complete bifurcation analysis of planar conewise affine systems. *Analysis and Control of Chaotic Systems*, Volume 2, No. 1, 2009.
- Y. Zou and T. Küpper. Generalized hopf bifurcation emanated from a corner for piecewise smooth planar systems. *Nonlinear Analysis: Theory, Methods and Applications*, vol. 62(1), pp. 1-17, 2005.
- M. U. Akhmet and D. Arugaslan. Bifurcation of a non-smooth planar limit cycle from a vertex. *Nonlinear Analysis: Theory, Methods and Applications*, volume. 71, pp. 2723-2733, 2009.
- S. H. Strogatz. *Nonlinear Dynamics and Chaos: with Applications to Physics, Biology, Chemistry, and Engineering*. Westview Press, 2001.